https://doi.org/10.5194/egusphere-2023-171
Preprint. Discussion started: 13 March 2023

A new multi-method approach for dating cave calcite: application to the cave of the Trou du Renard (Soyons, France)

Loïc Martin[1,2], Julius Nouet[3], Arnaud Dapoigny[1], Gaëlle Barbotin[2], Fanny Claverie [2], Edwige Pons-Branchu[1], Jocelyn Barbarand[3], Christophe Pécheyran[2], Norbert Mercier[4], Fanny Derym[5], Bernard Gély[6], Hélène Valladas[1]

[1]LSCE/IPSL, UMR 8212, CEA-CNRS-UVSQ, Université Paris-Saclay, Chemin de Saint Aubin - RD 128, F-91191 Gif sur Yvette Cedex, France
[2]Université de Pau et des Pays de l'Adour, E2S UPPA, CNRS, IPREM, Avenue de l'Université, BP 576 64012 PAU cedex, France
[3]Géosciences Paris Saclay, Université Paris-Saclay, CNRS, bâtiment 504, 91405 Orsay, France
[4]Archéosciences Bordeaux, UMR 6034 CNRS - Université Bordeaux Montaigne
Maison de l'archéologie, Esplanade des Antilles, 33607 PESSAC Cedex
[5]Site archéologique de Soyons, 28 rue de l'église, 07130 Soyons
[6]Service Régional de l'Archéologie de la région Rhône-Alpes, 6 quai Saint Vincent 69283 Lyon cedex

Correspondence to: Loïc Martin (loic.martin@glasgow.ac.uk)

Abstract. A multi-method approach aimed at characterizing carbonate parietal deposits and at proposing a chronology for these carbonate crusts is described. Dating was performed by radiometric methods (C-14 for recent samples, and U-series) on samples that had been characterized beforehand using optical and cathodoluminescence microscopy, and Fourier Transform Infrared microspectroscopy. For U-series, high precision on U-Th ages was achieved using liquid phase multicollector-ICP-MS applied to large samples, while laser-ablation single collector - ICP-SFMS provided information on the reliability of the sampling with a high spatial resolution. This methodology, based on the combination of these two techniques reinforced by the information obtained by the calcite characterization methods, was applied to carbonate deposits from the cave of the Trou du Renard (Soyons, France). The ages obtained with the two U-Th dating techniques are comparable and illustrate that different laminae were deposited at different rates in the samples. In the future, this procedure based on the mineralogical and geochemical characterization of the samples and their dating by radiometric methods will be applied to the layers of parietal carbonates deposited on Palaeolithic decorated walls. When the crystallization is slow, the U/Th dating method by imaging technique is of interest as well as that by multicollector-ICP-MS in liquid phase. The development of robust dating methods on very small quantities of material will make it possible to define the chronological framework of cave rock art.

1 Introduction

Establishing the chronology of cave art is a fundamental objective of studies on the cultural evolution of past societies. In Western Europe, and particularly in France, decorated caves are abundant but most of them have yielded figures consisting

https://doi.org/10.5194/egusphere-2023-171
Preprint. Discussion started: 13 March 2023

of engravings or made with metal oxides that cannot be dated directly. Nevertheless, the fact that many decorations are covered with carbonate deposits that can be dated by radiometric methods opens a new field of investigation for research on cave art since these deposits can, if they are not too old, be dated by the 14C method (Sanchidrian et al. 2017) but also by the U-series method (Valladas et al., 2017). However, with the latter , the main difficulty lies in the possible opening of the geochemical system in the event of detrital contamination by the surrounding sediments, or in the event of carbonate alteration accompanied by leaching of uranium (Perrin et al., 2014; Scholz et al., 2014, Pons-Branchu et al., 2020). In order to evaluate these phenomena that can affect carbonate deposits, and hence the U-Th ages, our objective here was to set up an experimental procedure combining different characterization and dating methods. We first tested this procedure on a cavity without any decorated elements where sampling could not deteriorate rock art.

The procedure must necessarily consider two important points. Firstly, in the context of prehistoric cave art, which is subject to preservation imperatives, it is necessary to be able to minimize the impact of the study, and therefore to optimize the sampling, while seeking to obtain a maximum of information. Secondly, to ensure the reliability of the results, it is important to assess the geological and archaeological context, which requires knowledge of the nature of the carbonate mineral and its evolution over time. For this purpose, we undertook petrographic analysis including optical and cathodoluminescence (CL) microscopy, and Fourier Transform Infrared microspectroscopy (µ-FTIR).

To test the relevance of this approach, we sampled two fragments of carbonate covering the wall of the Pillar Room in the "Trou du Renard" cave (Caves of Soyons, France), and a fistula fragment from the same room. Firstly, the petrography of each sample was determined. Secondly, quantitative multi-element mapping using a femtosecond laser ablation system coupled to a single collector sector field ICPMS (fsLA-single collector-ICP-SFMS), was carried out. High spatial and temporal resolutions were achieved on several samples and sub-samples, thus improving the understanding of calcite deposition on the cave walls. Subsequently, the carbonate samples were dated by the U-series disequilibrium method (U-Th) using two techniques: 1) Liquid phase - Multi Collector – Inductively Coupled Plasma Mass Spectrometry (Liq-MC-ICPMS) on dissolved and purified samples (following Pons-Branchu et al. 2020) and 2) a more recent approach based on U-series disequilibrium imaging using fsLA-single collector-ICP-SFMS (following Martin et al., 2022). The 14C dating method using the accelerator mass spectrometry (AMS) technique was also used for the most recent sample. This experimental procedure, combining the characterization of the nature of the carbonate itself and of its constitution, made it possible to obtain information on its temporal evolution, to compare the dating results and to discuss their reliability. This approach thus highlights the contribution of each method, as well as the advantage offered by their combination.

2 Materials and methods

2.1 From the sampling in situ to sample processing

The Trou du Renard cave, located in the southeast of France in the middle part and on the right bank of the Rhone valley, is composed of two main galleries: the Double-Borne network, where all the studied samples were taken from, and the Ursus

https://doi.org/10.5194/egusphere-2023-171
Preprint. Discussion started: 13 March 2023

network. It is part of a Jurassic Kimmeridgian karstic network presenting six other caves including the Moula-Guercy cave (Cailhol & Audra, 2013), which is well known for the unearthing of remains of cannibalized Neanderthals (Defleur et al., 1999). Although no human remains were found in the Trou du Renard cave, paleolithic fauna remains are present as well as two Mousterian flint flakes discovered in the Ursus network (Argant, 2010).

Three calcite samples from the Trou du Renard cave were analysed. The first sample (SOY19-01) is a fistula fragment that fell naturally from the ceiling of the Pillar Room between 2009 and 2010. The second and third samples, designated SOY19-02 and SOY19-03 respectively, are carbonate layers deposited on the wall of the Pillar Room. The sampling site corresponds to a place in the wall that is partially broken, where work has been undertaken to join a lower gallery (Fig 1.a). Sample SOY19-02 fell easily on the ground during sampling. Sample SOY19-03 was manually detached from the wall using a small electric saw, right next to the position of SOY-19-02. Given the proximity of these two samples (SOY19-02 and SOY19-03), they can be considered to represent the same depositional levels and, in each of them, two carbonate layers separated by a clay film were distinguished. The resulting sub-samples were then designated as SOY19-02 Exo and SOY19-03 Exo for the external parts (surface side), and SOY19-02 Endo and SOY19-03 Endo for the internal part (Fig 1.b). We decided to concentrate our efforts on a single sample and to perform most of our investigations on SOY19-02 and only a few on SOY19-03 in order to compare the respective characteristics of the two samples. Sample SOY19-01 and the two sub-samples of SOY19-02 were then split into several pieces to allow for the different analyses.

Figure 1: Samples SOY-19-02 and SOY-19-03

(a) view of the sampling area.

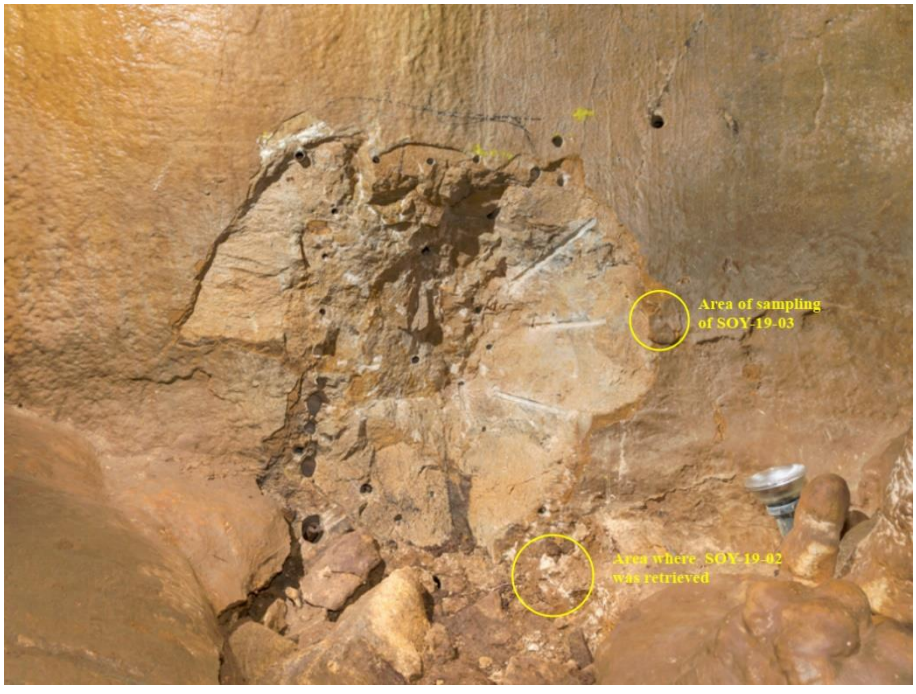

https://doi.org/10.5194/egusphere-2023-171
Preprint. Discussion started: 13 March 2023

(b) preparation of sample SOY-19-02 for analyses.

2.2 Petrographic analysis

Each sample was prepared for the realization of thin slides and epoxy resin blocks. Slides were observed by optical and cathodoluminescence microscopy, while resin blocks were used for FTIR imaging after polishing. Microscopic images of the samples were acquired using a Leica microscope under plane polarized light (PPL) at a magnification of x25. Cathodoluminescence (CL) imaging was carried out using a Newtec cold cathode system operating at ~10 kV and ~250 µA coupled to a BX41 Olympus microscope at a magnification of x25. The images were modified using retouching software to increase contrast and colour.

Fourier Transform-Infrared images were acquired using a Spotlight 400 FT-IR imaging system coupled with a Frontier IR spectrometer, both from Perkin Elmer, in reflection mode on polished surfaces. Rapid scans of SOY19-02 and SOY19-03 confirmed the high similarity between these samples. High resolution FT-IR scans of the sub-samples Endo and Exo of SOY19-02 were then performed. Four absorption bands are observable in carbonates: a broad high intensity band (1500-1400 cm-1), two broad medium intensity bands (1100-1000, 900-800 cm-1) and a very weak absorption band near 700 cm-1 (Andersen and Brečević, 1992). The band at 900-800 is called v2 and the band near 700 cm-1 is called v4. The v4 band and the band at 1500-1400 cm-1 are split into two smaller bands. The position of the v2 band distinguishes the different carbonate minerals: calcite (874-878 cm-1), aragonite (853-859 cm-1), dolomite (881 cm-1) and magnesite (887 cm-1) (Huang and Kerr, 1960; Andersen and Brečević, 1992 and references therein). The position of these bands is indicative as the data produced in this study correspond to reflection bands.

https://doi.org/10.5194/egusphere-2023-171
Preprint. Discussion started: 13 March 2023

2.3 Mapping of elements

After petrographic analysis, the resin block samples were recut to fit the femtosecond laser ablation cell, and the sections were polished in order to obtain a flat surface for ablation. Elemental mappings via ^{238}U, ^{232}Th, ^{27}Al, ^{24}Mg and ^{43}Ca isotopes were obtained using high repetition rate 257 nm UV femtosecond Laser Ablation (Lambda 3, Nexeya, Pessac, France) coupled to a single collector sector field ICP-MS fitted with a jet interface (Element XR, Thermo Fisher, Bremen, Germany). The samples were ablated at a repetition rate of 1000 shots per second using a combination of two simultaneous movements: on the one hand, a vertical back-and-forth laser beam movement of 50µm at a speed of $1mm.s^{-1}$ allowed by 2 galvanometric scanners fitted into the laser machine and on the other hand, the movement of the X-Y stage supporting the sample consisting in successive lines with 50µm spacing at a speed of $50µm.s^{-1}$. The number of counts per mass was read per cycle of 1s, resulting in a final reconstructed image of 50 µm square pixels. Image sizes ranged from 5.5mm to 8.4mm, and each took from 4h to 6h of measurement. ^{238}U was mapped in order to investigate the uranium distribution in the samples, while ^{232}Th mapping was used to evaluate the potential detrital correction that needed to be applied to U-series disequilibrium dating. The ^{27}Al and ^{24}Mg elements were considered as proxies of clay or sediment deposit in the samples. ^{43}Ca was measured as the proxy of carbonate in the sample.

2.4 U-Th dating methodology

2.4.1 Liq-MC-ICPMS

The complete protocol used to prepare the samples, measure isotopic ratios and calculate ages is described in Pons-Branchu et al. (2014). Sub-samples of SOY19-01 and SOY19-02 Exo and Endo were cut in the laboratory using a rotary micro-saw. Two samples (internal and external) were extracted from SOY 19-01, one from the SOY19-02 Exo sample and two (internal and external) from the SOY 19-02 Endo sample. They were weighed (between 68 and 167 mg) in PFA Teflon™ beakers where a known amount of ^{229}Th-^{236}U spike calibrated against the HU-1 uraninite assumed to be at secular equilibrium, had been previously added. Then the separation of U and Th fractions was performed on U-TEVA resin in nitric media. The isotopic ratios were measured with a Neptune-plus MC-ICPMS fitted with a jet pump interface and an Aridus II desolvating system.

2.4.2 fsLA-single collector-ICP-SFMS

The resin indurated samples were used for direct U-Th dating by high-sensitivity and high-resolution fsLA-single collector-ICP-SFMS mapping of ^{238}U, ^{234}U, ^{230Th} and ^{232}Th. The details of the dating protocol are described in Martin et al. (2022). Mappings of SOY19-01, SOY19-02Endo and SOY19-02Exo with sizes of $5.4x1.35mm^2$, $4.2x4.8mm^2$, and $2.79x3.3mm^2$ respectively, were made with a resolution of 50 µm. Each mapping includes the measurement of a blank for 30 minutes before and after sample ablation. Spatial variations in ^{238}U content and $^{232}Th/^{238}U$ ratio were used to define several "*Regions*

https://doi.org/10.5194/egusphere-2023-171
Preprint. Discussion started: 13 March 2023

Of Interest" (ROI) on the SOY19-02 mappings, potentially corresponding to different periods of calcification. The isotope ratios used for U-Th dating were calculated for each of the ROIs.

2.4.3 Detrital corrections

Three approaches were used for U-Th dating. The first one was based on an *a priori* $^{230}Th/^{232}Th$ value for the detrital fraction, here an activity ratio of 1.50 ± 0.75 which is the common value used for speleothems (Hellstrom 2006). The second approach was used for the results obtained using fsLA-single collector-ICP-SFMS. Since this method enables several ages to be obtained on the same section, with clear stratigraphic positions, the corrected ages can be modelled using stratigraphic constraints: a large range of $^{230}Th/^{232}Th$ values for the detrital fraction are tested for age corrections, and the model keeps those that give ages in stratigraphic order after correction. Here we used the STRUTAge routine (Roy-Barman and Pons-Branchu, 2016).

2.5 ^{14}C dating

A sub-sample of SOY-19-01 of about 10 mg was taken using a rotating micro-saw for ^{14}C analysis. It was hydrolysed with H_3PO_4 to obtain CO_2 and converted to graphite (Dumoulin et al., 2017) for measurement at the Artemis AMS-French National facility (CEA Saclay, LMC14; Moreau et al., 2020). Carbon isotope ratios were corrected for isotopic fractionation based on $\delta^{13}C$ values measured on the AMS, following international recommendations (Mook and van der Plicht, 1999). The ^{14}C results were calibrated using Intcal20 (Reimer et al. 2020) with no correction for the proportion of dead carbon (DCP), and with corrections for different DCP (5, 10 and 20%, see table 2), following Sanchidrian et al. (2017). They are presented in table 2.

3 Results

3.1 Petrography and mapping results

The section of the fistula shows a radial structure with two homogeneous crystallization domains: a central dark domain and a peripheral main domain consisting of successive layers of carbonate (Appendix A, Fig A1). The passage between the two domains is marked in CL by a red band while the rest of the sample is non-luminescent. The mineralogy is homogeneous with a position of the v2 band characteristic of poorly crystallized (Full Width at Half Maximum: FWHM >10 cm^{-1}) calcite (875-878 cm^{-1}).

The carbonate levels sampled for SOY-19-02 and SOY-19-03 consist of thin layers that appear very dark under optical microscopy, alternating in places and mainly in the outer part with layers made of larger crystals (Fig 2.a and Appendix A, Fig A2.a). The growth is quite regular and shows well developed carbonate veils. The CL image confirms this relative

https://doi.org/10.5194/egusphere-2023-171
Preprint. Discussion started: 13 March 2023

homogeneity of the sample with mainly non-luminescent carbonates (blue light in Fig 2.b and Appendix A, Fig A2.b) and some levels with red luminescence.

Figure 2: Images of the SOY-19-02 sample in optical PPL microscopy and CL microscopy. Magnification is x25.

(a) optical PPL microscopy

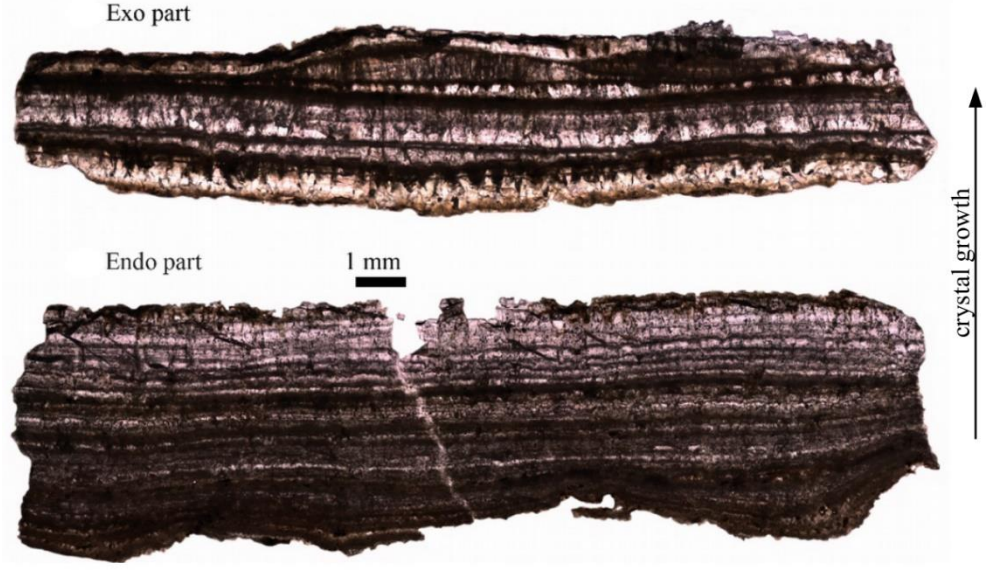

(b) CL microscopy

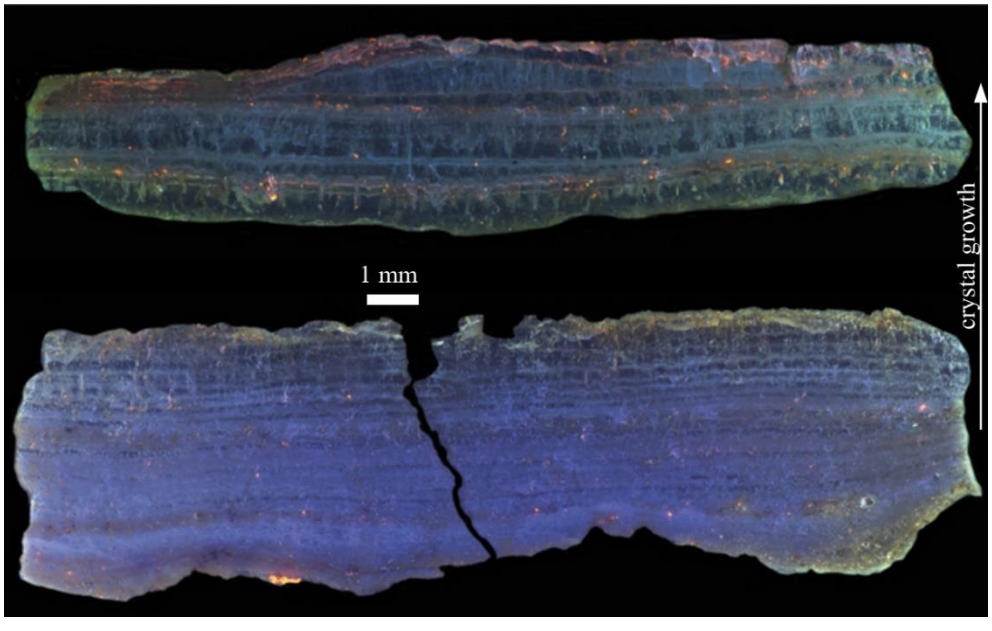

https://doi.org/10.5194/egusphere-2023-171
Preprint. Discussion started: 13 March 2023

Figure 3: FT-IR analysis of SOY-19-03. The position of the v2 band is represented on the left while the full width at half-maximum of the v2 band is on the right. The Exo part is at the top of the images.

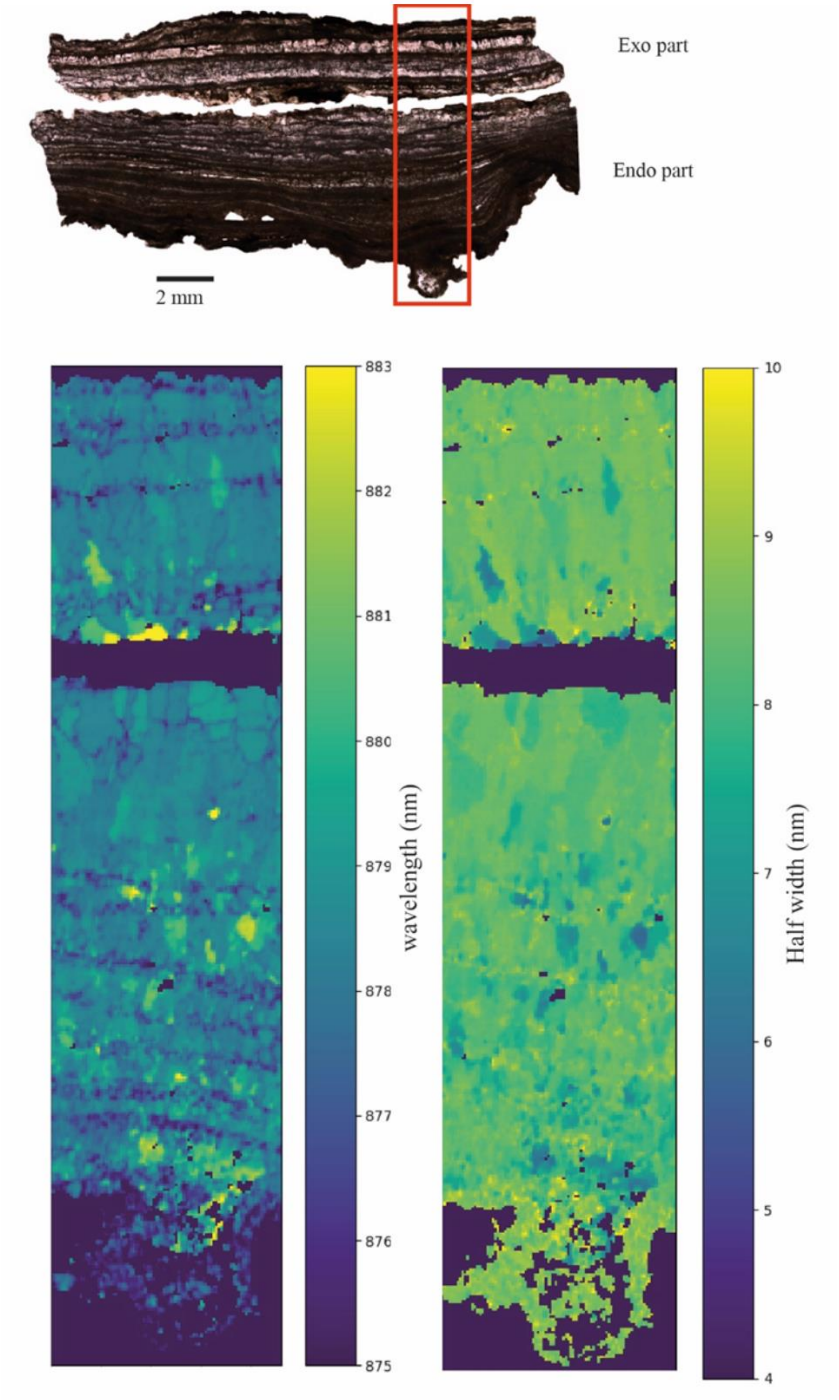

https://doi.org/10.5194/egusphere-2023-171
Preprint. Discussion started: 13 March 2023

The FT-IR image shows that most of the sample is very homogeneous and consists of calcite crystals (v2 band between 876 and 880 cm^{-1}) which are well crystallized (FWHM < 10 cm^{-1}) (fig. 3). Some minor components show a different FT-IR signal with a higher wavenumber, especially at the interface between the Endo and Exo sub-samples (Fig 3). This difference in spectroscopic signatures may be linked to cation divalent substitution. A similar but larger displacement of the v2 band is indeed interpreted as an increase in substituted Mg along the solid solution between calcite, dolomite and magnesite (Huang and Kerr, 1960).

The fsLA-single collector ICP-SFMS mappings of SOY19-02 Endo indicate a good homogeneity of the distribution of the chemical element investigated (^{24}Mg, ^{27}Al, ^{238}U, ^{232}Th and ^{43}Ca), apart from the basal part (at the top of the images) which corresponds to a mixture between the substrate and the calcite deposit (Fig 4). Mappings highlight the more pronounced presence of detrital layers between the calcite layers in SOY19-02 Exo, identified in particular by a higher Al and Mg contents. It is noticeable that a large Al and Mg rich zone is visible at the root of SOY19-02 Endo, which corresponds to a piece of the limestone host rock. The ^{238}U and ^{232}Th values show a good correlation with the presence of detrital layers. This was confirmed by the additional measurement of uranium and thorium isotopes required for U-Th dating and was considered by correcting the ages from the detrital ^{230}Th fraction (Table 1, Fig 9).

Figure 4: FsLA-quad-ICPMS qualitative mappings of ^{24}Mg, ^{27}Al ^{238}U, ^{232}Th and ^{43}Ca in sample SOY-19-02. Signals are in counts per seconds second (cps). This slice presents the Endo part at the bottom and Exo part at the top.

(a) ^{24}Mg

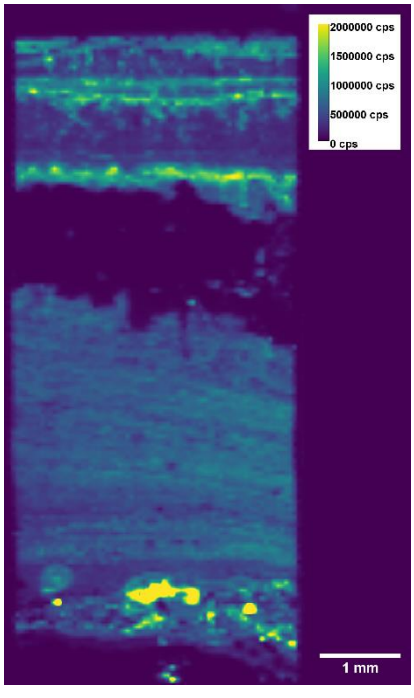

(b) ^{27}Al

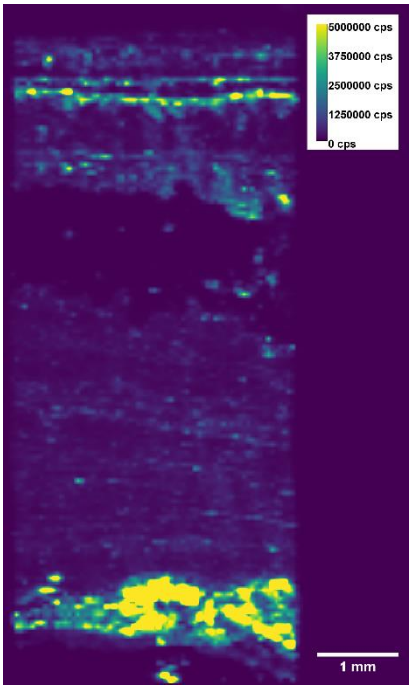

https://doi.org/10.5194/egusphere-2023-171
Preprint. Discussion started: 13 March 2023

(c) ^{238}U

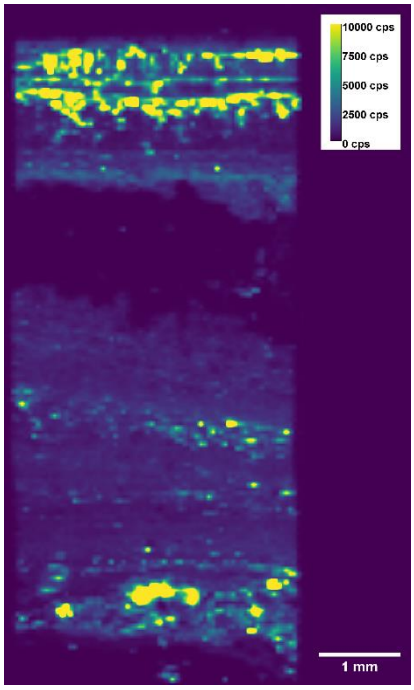

(d) ^{232}Th

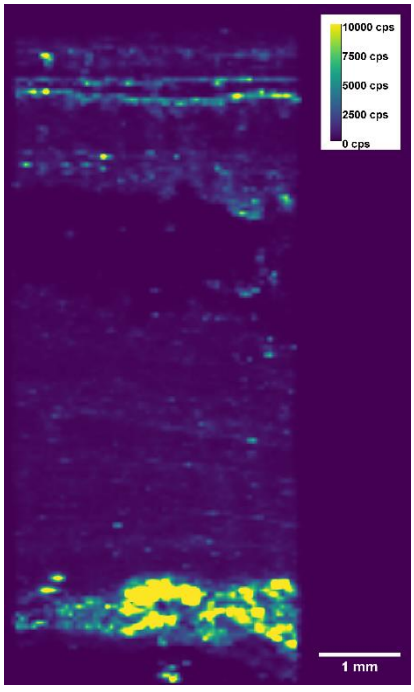

(e) ^{43}Ca

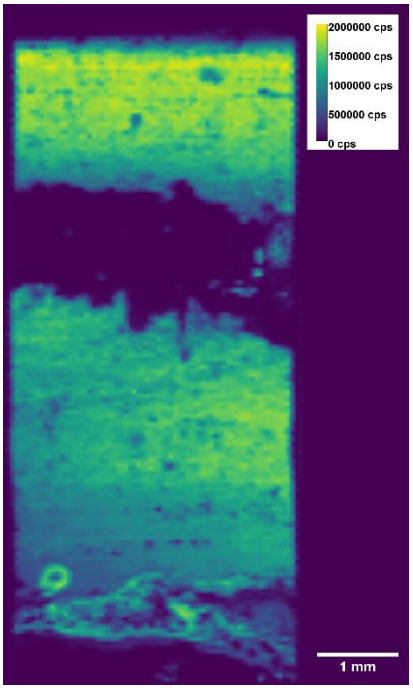

https://doi.org/10.5194/egusphere-2023-171
Preprint. Discussion started: 13 March 2023

In conclusion, data from different analytical methods converge towards a coherent description of the samples. They all are composed of successive layers of pure calcite, without any evidence of diagenesis (Fig 2 and Fig 3). The detrital fraction, highlighted by the presence of Mg and Al in the fLA-single collector-ICP-SFMS images, is significant and varies between the different layers (Fig 4).

3.2 Dating results

The different U-Th ages obtained by Liq-MC-ICPMS and by fsLA-single collector-ICP-SFMS imaging are presented in Table 1. ^{14}C dating results of SOY-19-01 are given in Table 2. Figure 6 depicts all the chronological data obtained, before and after the detrital correction of the U-Th ages.

3.2.1 Liq-MC-ICPMS

^{238}U contents range from 0.198 ± 0.002 to 0.953 ± 0.008 ppm, and ^{232}Th contents from 0.257 ± 0.002 and 140 ± 1 ppt. $^{230}Th/^{232}Th$ activity ratios, from 5.3 ± 0.2 to 39.9 ± 1.3 suggest that correction for detrital thorium is not negligible. The use of an *a priori* value for isotopic thorium composition of the detrital phase with a 50% uncertainty led to the notable increase of error bars for corrected ages. They range from 187.9 ± 5.3 ka to 1.4 ± 0.1 ka.

3.2.2 fsLA-single collector-ICP-SFMS

The fsLA-single collector-ICP-SFMS provided qualitative mappings of ^{230}Th, ^{232}Th, ^{234}U and ^{238}U with relative variations. They confirmed the observation from sample characterization. SOY-19-02 Endo and SOY-19-01 appear relatively homogeneous, while distinct successive layers can be observed on SOY-19-02 Exo. Mappings of the ^{238}U signal and the $^{232}Th/^{238}U$ ratio for the different samples are presented in Appendix B. These mappings were used to define "*Regions Of Interest"* (ROIs) corresponding to different calcite layers, according to Martin et al. (2022) and as shown in Fig 5. The small variations in ^{238}U content and $^{232}Th/^{238}U$ ratio for sample SOY19-01 did not allow such ROIs to be defined and therefore only one age was calculated. No significant difference of raw age was observed for SOY-19-02 Endo, meaning that the duration of the formation of the sample is below the age resolution of the method. Consequently, only one U-Th age was calculated for this sample using fsLA-single collector -ICP-SFMS mapping.

The detrital-rich layers identified by their Al content correspond to higher raw ages before detrital correction (Fig 6). In particular, layers 1, 3 and 7 of SOY-19-02 Exo present the highest $^{232}Th/^{238}U$ ratios (Fig 5) and their uncorrected ages result in a chronological inversion with respect to the less detritus-rich layers, including the Endo part. However, when corrected for the detrital ^{230}Th fraction, their ages are coherent with the order of deposition of these layers using correction with an *a priori* value of the detrital fraction, and obviously using correction assuming stratigraphic constrains (fig.6). Note that the initial $^{230}Th/^{232}Th$ activity ratio for the detrital fraction as determined by the STRUTages routine (Roy-Barman and Pons-Branchu, 2016) is 1.72 ± 0.30, very close to the a priori value used (1.5 ± 0.75).

https://doi.org/10.5194/egusphere-2023-171
Preprint. Discussion started: 13 March 2023

Figure 5: definition of the different layers of SOY-02Exo on the $^{232}Th/^{238}U$ ratio mapping obtained by fsLA-single collector-ICP-SFMS. The layer numbers are indicated on the figure, starting from 1 for the layer in contact with the Endo part to 7 for the surface layer. The ages on the left are the STRUTages computed according to Roy-Barman and Pons-Branchu (2016)

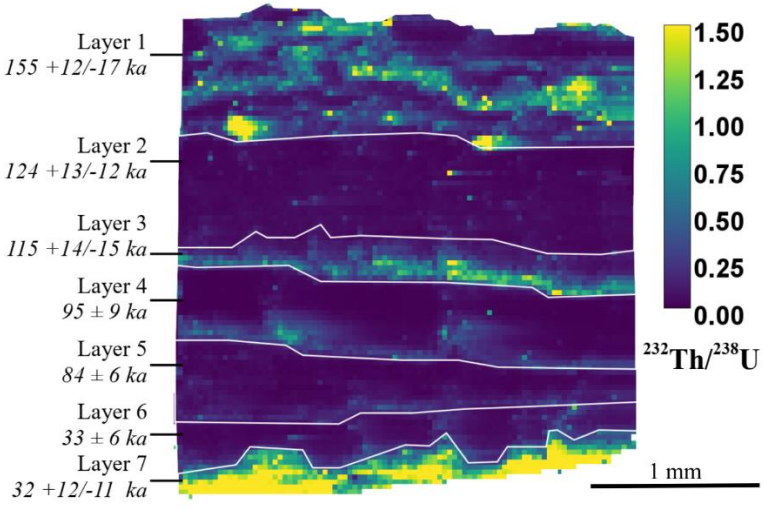

Figure 6: Comparison of the U-Th ages obtained for samples SOY19-01 and SOY19-02 by the liq-MC-IPMS and by fsA-SC-ICP-SFMS techniques.

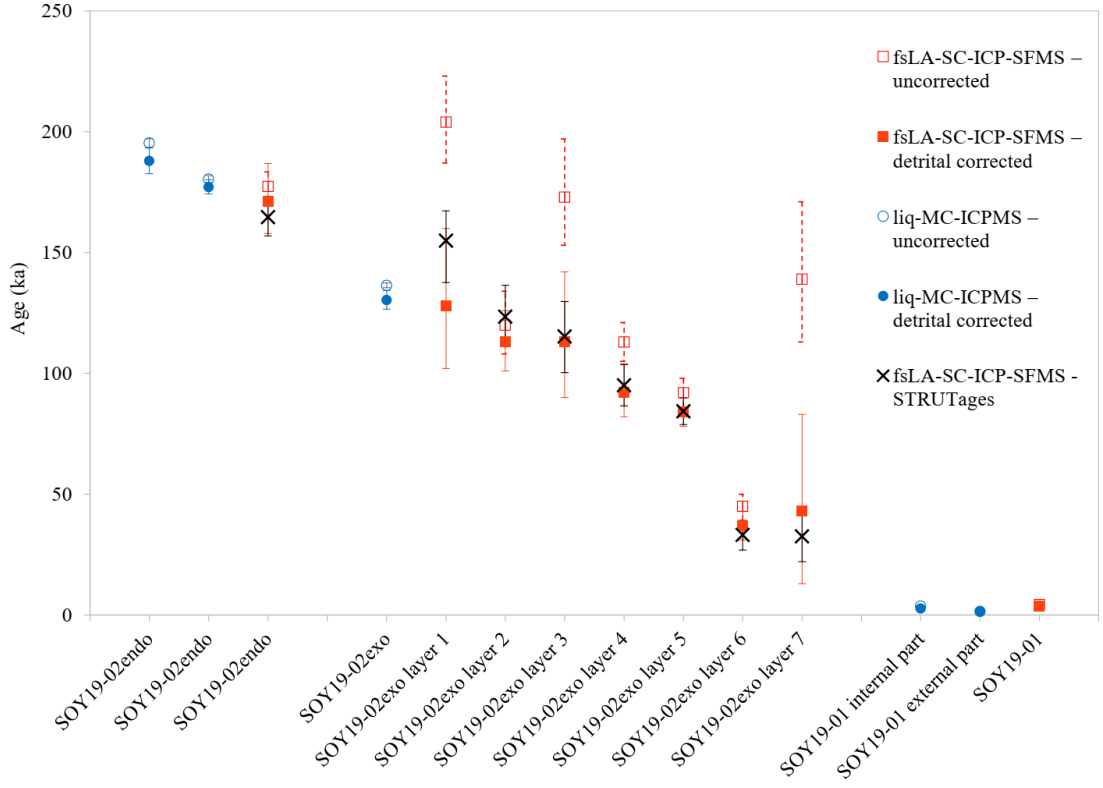

https://doi.org/10.5194/egusphere-2023-171
Preprint. Discussion started: 13 March 2023

Table 1: U-Th dating results. U and Th contents (columns 4-6), activity ratios (columns 7 and 8), ages (ka) uncorrected for detrital content (column 9). corrected ages at 2 sigma (column 11) for detrital content, expressed as years before 1950 (BP), assuming a $^{230}Th/^{232}Th$ ratio of 1.5 ± 50%. In column 11, the corrected ages* computed according to stratigraphic constraints (with samples Endo bulk and Exo layers 1 to 7), using the STRUT ages routine are given in italics (Roy-Barman and Pons-Branchu 2016). Results are given for strict coeval constraints, with 30% variability for Ri = $(^{230}Th/^{232}Th)_{det}$ determined here at 1.72 ± 0.3

Sample	Sub-sample	Method of analysis	^{238}U (ppm)	^{232}Th (ppb)	$\delta^{234}U_M$ (‰)	$^{230}Th/^{238}U$	$^{230}Th/^{232}Th$	Age (ka)	$\delta234U_T$ (‰)	Detrital corrected age (ka)
SOY19-02	Endo-1	Liq-MC-ICPMS	0.687 ± 0.005	132 ± 1	189.4 ± 0.9	1.027 ± 0.003	16.31 ± 0.04	195.3 ± 1.8	322.1 ± 5.1	187.9 ± 5.3
	Endo-2		0.494 ± 0.004	39.4 ± 0.3	180.8 ± 0.9	0.9773 ± 0.002	37.38 ± 0.07	180.4 ± 1.4	282.9 ± 3.1	177.2 ± 3.0
	Endo bulk	fsLA- single collector-ICP-SFMS			178 ± 8	0.98 ± 0.01	18.1 ± 0.2	177 ± 6	279 +27/-24	163 +17/-15 *165 +7/-8**
	Exo bulk	Liq-MC-ICPMS	0.953 ± 0.008	140 ± 1	171.5 ± 1.2	0.865 ± 0.003	17.95 ±0.05	136.4 ± 1.0	261.4 ± 3.2	130.4 ± 3.9
	Exo layer 1	fsLA-single collector-ICP-SFMS			184 ± 18	1.05 ± 0.03	7.8 ± 0.2	204 +19/-17	269 +51/-41	128 +32/-26 *155 +12/-17**
	Exo layer 2				190 ± 30	0.82 ± 0.05	50.2 ± 2.8	120 +14/-12	262 +53/-49	113 +13/-12 *124 +13/-12**
	Exo layer 3				240 ± 30	1.02 ± 0.05	7.7 ± 0.4	173 +24/-20	334 +72/-60	113 +29/-23 *115 +14/-15**
	Exo layer 4				227 ± 20	0.81 ± 0.03	12.9 ± 0.5	113 ± 8	297 +36-33	92 +12/-10 *95 ± 9**
	Exo layer 5				230 ± 18	0.71 ± 0.03	30.9 ± 1.1	92 ± 6	293 +29/-28	84 ± 6 *84 ± 6**
	Exo layer 6				266 ± 36	0.43 ± 0.04	10.4 ± 0.9	45 ± 6	296 +45/-44	37 ± 6 *33 ± 6**
	Exo layer 7				293 ± 58	0.96 ± 0.09	2.7 ± 0.3	139 +32/-26	252 +111/-88	43 +40/-30 *32 +12/-11**
SOY19-01	int	Liq-MC-ICPMS	0.198 ± 0.002	0.257 ± 0.002	94.9 ± 2.0	0.0366 ± 0.0010	5.3 ± 0.2	3.7 ± 0.1	95.6 ± 2.0	2.7 ± 0.6
	ext		0.218 ± 0.002	4.157 ± 0.034	120.4 ± 1.6	0.0153± 0.0005	39.9 ± 1.3	1.5 ± 0.1	120.9 ± 1.6	1.4 ± 0.1
	bulk	fsLA-single collector-ICP-SFMS			87 ± 23	0.04 ± 0.01	8.4 ± 2.6	4.3 ± 1.3	88 ± 23	3.6 ± 1.5

**STRUTages calculated ages (Roy-Barman and Pons-Branchu 2016)*

https://doi.org/10.5194/egusphere-2023-171
Preprint. Discussion started: 13 March 2023

Table 2: Results of ^{14}C analyses for sample Soy-19-01-int, presented as percent of Modern Carbon (pMC), uncalibrated and calibrated ages (assuming 0 and 10% of DCF) using IntCal20 atmospheric curves (Reimer et al., 2020) with OxCal 4.2 software (Bronk Ramsey, 1995).

Lab cod	Ech		$\delta^{13}C$	pMC	Years BP	Year Cal BP with 0% DCP	Year Cal BP with 5 % DCP	Year Cal BP with 10% DCP	Year Cal BP with 20% DCP
Sac - 64947	Soy-19-01-int		-14.40	75.177 ± 0.207	2290 ± 30	2351 - 2181	1863 - 1724	1365 - 1301	541 - 510

3.3 Comparison of U-Th results obtained by the two techniques

3.3.1 The Endo part of SOY-19-02

Two levels (internal and external part) were analysed in this thick sample using Liq-MC-ICPMS at 187.9 ± 5.3 ka and 177 ± 3.0 ka, hence a weighted mean at 179 ± 5 ka BP. Using fsLA-single collector-ICP-SFMS, a single age was calculated since the sample is very homogenous (Fig 4). The result, 163 +17/-15 or 165 +7/-8 depending on the correction used for the detrital fraction, is in agreement with the results obtained using the other technique (Table 1 and Fig 6).

3.3.2 The Exo part of SOY-19-02

Liq-MC-ICPMS gave a single age for the bulk sample of 130.4 ± 3.9 ka (corrected for the detrital content), whereas 7 successive layers were identified and dated using fsLA-single collector-ICP-SFMS. The STRUT ages obtained for layers 1 to 5 ranged from 155 +12/-17 to 84 ± 6 ka BP (Table 1 and Fig 6). The chronological gap between layers 5 and 6 (33 ± 6 ka) may be due to drier conditions in the cave during this time interval (MIS4). The small age difference between layers 6 and 7 may be due to a higher calcite deposition during MIS3.

3.3.3 SOY-19-01 sample

Two levels were analysed in this thick sample using Liq-MC-ICPMS with corrected age from 2.7 ± 0.6 and 1.4 ± 0.1 ka (weighted mean 1.7 ± 0.4 ka BP). This mean age is consistent with the single value obtained using fsLA-single collector-ICP-SFMS at 3.6 ± 1.5 ka, and with the ^{14}C age (1.36-1.30 ky) of this sample assuming a proportion of dead carbon of up to 10% (Table 1 and Table 2).

3.3.4 Summary of ages obtained by comparing the two techniques

Table 1 and Figure 6 show that the precision of the measurements made with the Liq-MC-ICPMS protocol is significantly better than those made with the fsLA-single collector-ICP-SFMS protocol. While the former is a well-established protocol (Pons-Branchu et al., 2014), the latter is more recent (Martin et al., 2022) and further experimental work is certainly needed to improve its precision. However, most of this difference is related to the mass sampled per analysis (68 to 167 mg for the Liq-MC-ICPMS protocol compared to only 1 to 3 mg for the fsLA-SC-ICPMS protocol) and to the multicollector system

https://doi.org/10.5194/egusphere-2023-171
Preprint. Discussion started: 13 March 2023

used for the Liq-MC-ICPMS measurements, which offers greater counting statistics and hence greater precision in the determination of isotope ratios than a sequential system such as fsLA-single collector-ICP-SFMS. Note that the mass sample used for the Liq-MC-ICPMS protocol can also be reduced: here large pieces of samples were used because the U content was not known before the analysis. While the precision of the fsLA-single collector-ICP-SFMS ages could be increased by capturing additional images, which would therefore correspond to an increase in the mass analysed, the cost and time required to achieve the same level of precision as the Liq-MC-ICPMS protocol would be very high.

The refinement of the chronology by the STRUT ages method significantly improved the precision of the fsLA-single collector-ICP-SFMS U-Th ages, although the ages by Liq-MC-ICPMS are still more precise. Combining a high spatial resolution of ages with stratigraphical constraints has a strong potential for improving the chronological data of cave deposits.

The spatial resolution of the fsLA-single collector-ICP-SFMS analysis also offers new insights into the dating of complex samples: the possibility of sampling individual layers and calculating their ages allows the rate of formation of the carbonate deposits to be estimated. On the contrary, it is noticeable that when successive layers with an age difference greater than the age resolution of the dating method are analysed in bulk, as in the case of sample SOY-19-02Exo (Table 1 and Fig 6), the apparent age obtained may not represent the average age of the layers but an average value weighted by the amounts of U-series elements present in each layer of the sub-sample. Consequently, the thickest and most U-enriched layers will have a greater weight on the apparent age compared to the other layers. The ability to identify the different layers for age calculation avoids this possible bias and thus improves the understanding of the calcite deposition process. In addition, the mapping of isotopes and isotope ratios can be used to identify areas affected by detrital incorporation, and to calculate an age correction, or alternatively, to check that the usual value for detrital correction is relevant. Uranium leaching can also be highlighted, and areas affected by these changes can be excluded from the age calculation.

In sum, it appears that the two techniques (Liq-MC-ICPMS and fsLA-single collector-ICP-SFMS) for U-Th dating are complementary, each with its own advantages and disadvantages.

4 Implication for rock art studies

For several years, the carbonated layers deposited on decorated walls have been dated by the U/Th method (Pike et al. 2012): depending on their location above or below the parietal representation, their dating gives a terminus ante quem or a terminus post quem for the decoration respectively. However, the reliability of some U/Th dating results has been questioned because no attention was paid to the uranium behaviour as a function of time and its possible mobility, which would invalidate the dating results. To ensure the validity of the dating results, we proposed in previous studies to use simultaneously U/Th and ^{14}C methods on the same carbonated sample and to compare their respective results (Plagnes et al., 2003; Valladas et al., 2017; Pons-Branchu et al., 2020). We also proposed to characterize and study the carbonate mineral and its geochemical evolution through time and to multiply the dating analysis to check the reliability of the results.

https://doi.org/10.5194/egusphere-2023-171
Preprint. Discussion started: 13 March 2023

In this work, the differences between the two techniques represent a great potential to improve U-Th dating: isotope imaging and the resulting in-situ dating could indeed be used to guide the micro-sampling for the Liq-MC-ICPMS protocol. For example, for the Exo part of sample SOY-19-02, the isotope imaging indicates the need to increase the micro-sampling to better match the successive layers observed, unlike the Endo part where there are small age differences between layers.

This study illustrates a case where the samples do not show evidence of major alteration and the ages obtained with the two U-series techniques, and with ^{14}C, agree. The control of the basic hypothesis on which the dating is based, such as the absence of diagenesis and the application of detrital correction, is a key element that only the approach we have implemented in this case study allows, and which ultimately leads to reinforcing the reliability and robustness of the chronology. Even in the event of alteration or disagreement on the chronology (between two different chronometers or regarding stratigraphic correction), our approach would allow the effect of alteration and the possible origins of disagreement to be investigated. This would allow errors to be corrected or would indicate if any further analysis was required.

In the present study, the initial size of the samples (a few cm) is not compatible with the preservation requirements for decorated caves. However, the total mass required for petrographic analysis and dating is only a fraction of this amount, less than one gram. In the context of Le Trou du Renard cave, the initial sampling was carried out with the aim of having sufficient mass to develop a multi-method analysis and dating protocol. The development of this protocol and the data obtained now allow a more accurate assessment of the amount of sampling required to establish a reliable chronology, as well as to envisage a sampling strategy compatible with the imperative of preservation of decorated caves. Similar analyses to this study can be carried out in non-decorated areas, or on small or naturally fallen pieces of calcite to establish a chronology of calcite deposition in the cave and to highlight any difficulties for dating methods. If discussed in relation to the archaeological, geological and preservation expertise, such results would probably allow the identification of sampling points closest to the decoration that would maximize the chronological data for a minimum of sampled mass, i.e. 1 to 10 mg of sample taken with a micro-drill tool.

5 Conclusion and prospective strategy

Studies carried out on prehistoric art in order to determine the cultural evolution of Palaeolithic populations require the establishment of a reliable chronology. It is thus essential to be able to control the validity of dating results obtained on carbonate parietal deposits and to check that they were not subjected to diagenesis processes.

Dating of calcite layers from the Trou du Renard cave walls (France) by the U-Th and ^{14}C methods revealed a long-term development of these deposits, between 187.9 ± 5.3 ka and 1.4 ± 0.1 ka.

Both U-Th dating techniques –liquid MC ICP-MS and fsLA-single collector-ICP-SFMS- agree on the chronology but lead to different precisions and resolutions. The ^{14}C age of the youngest sample is in agreement with the U-Th dating results. No evidence of diagenesis was detected from the petrographic (optical and cathodoluminescence microscopy and FTIR

https://doi.org/10.5194/egusphere-2023-171
Preprint. Discussion started: 13 March 2023

microspectroscopy) and geochemical mapping of selected chemical elements (Al, U, Th and Mg contents). The detrital incorporation of ^{230}Th was corrected for all U-Th ages and the dead carbon fraction was taken into account for the ^{14}C age.

More generally, the development of dating methods and associated technologies make it possible to use smaller sample sizes, as well as to improve the age precision and spatial resolution of analysis. These improvements allow for a better constraint and understanding of the chronology while reducing the impact of sampling on the site. Imaging methods provide geological and chemical data on samples to support the chronology, controlling several parameters such as sample homogeneity, presence of detrital phase and evidence of diagenesis (Spooner et al., 2016; Martin et al., 2022). U-Th dating using fsLA-single collector-ICP-SFMS imaging, while not reaching the precision of liquid MC ICP-MS U-Th dating, reveals information on the chronology of the deposits with a high spatial resolution. This could contribute to assessing the chronological relationship between dated calcite deposits and archaeological remains and to constraining their relative age when a calcite deposit over/underlies them. Combining the high precision of liquid MC ICP-MS U-Th dating with imaging methods could achieve the objective of maximizing chronological information from a reduced sample size, which is a necessary condition for the most sensitive archaeological sites. This study aimed at demonstrating the feasibility and advantages of this association.

https://doi.org/10.5194/egusphere-2023-171
Preprint. Discussion started: 13 March 2023

Appendix A: Images of the SOY-19-01 and SOY-19-03 samples in optical microscopy (plane polarized light) and cathodoluminescence (CL) microscopy

Figure A1: petrographic description of sample SOY-19-01. Left is optical microscopy and right is CL microscopy. Magnification is x25.

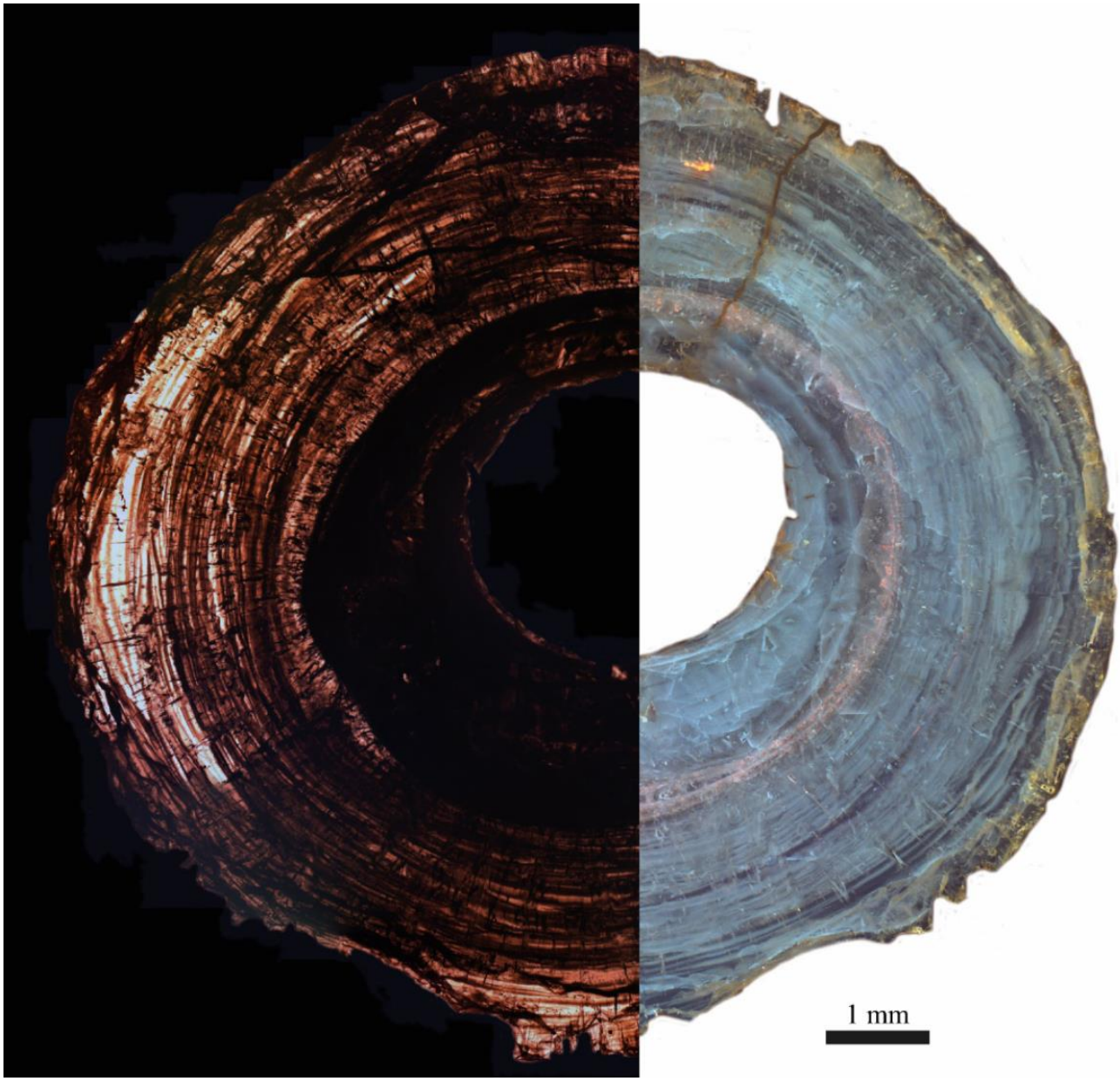

https://doi.org/10.5194/egusphere-2023-171
Preprint. Discussion started: 13 March 2023

Figure A2: petrographic description of sample SOY-19-03. Top is optical microscopy and bottom is CL microscopy Magnification is x25.

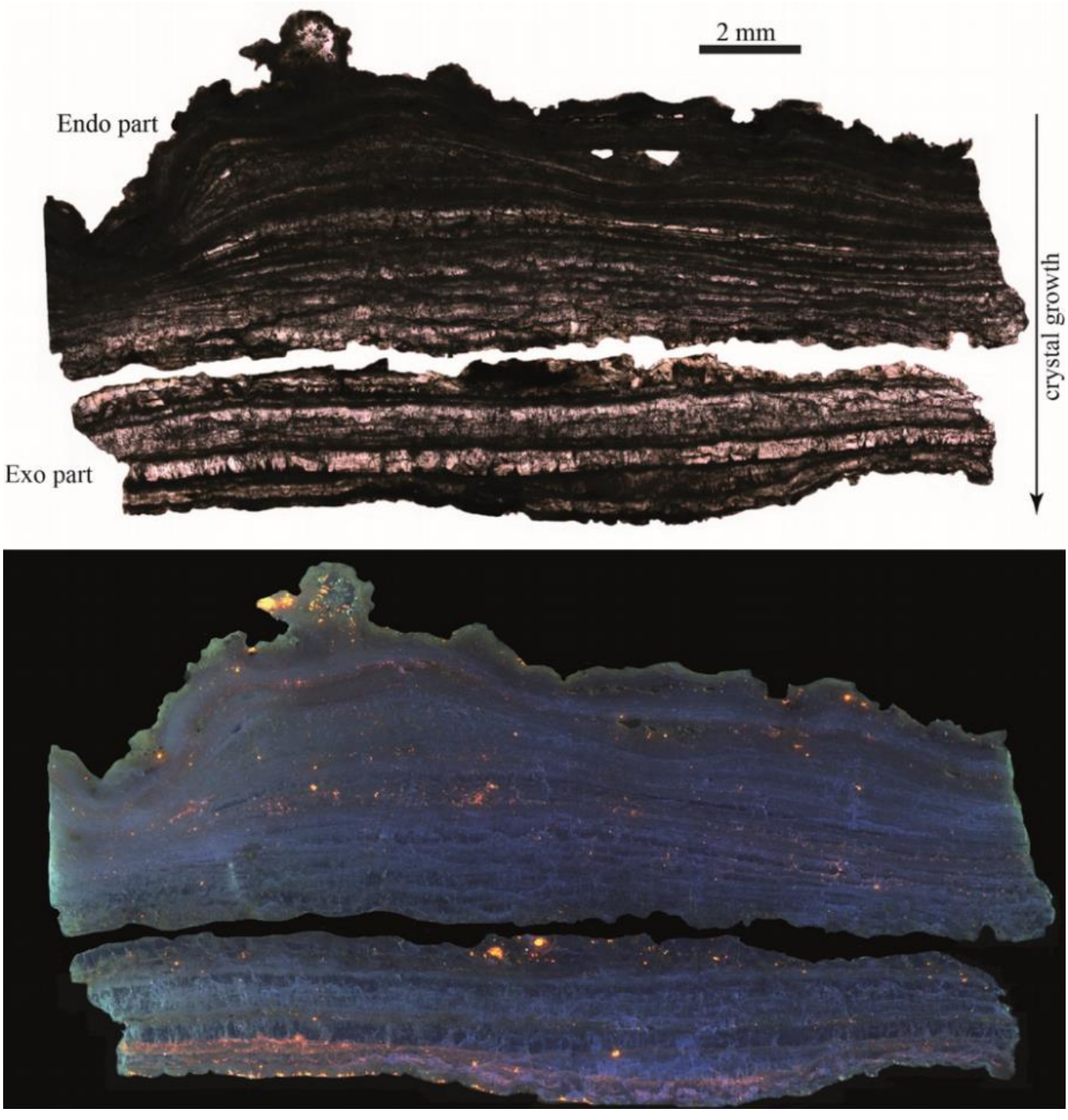

https://doi.org/10.5194/egusphere-2023-171
Preprint. Discussion started: 13 March 2023

Appendix B: fsLA-single collector-ICP-SFMS mappings of ^{238}U signal and of the $^{232}Th/^{238}U$ ratio for the different samples

Figure B1: sample SOY-19-01. The centre of the fistula is on the right of the images

(a) ^{238}U

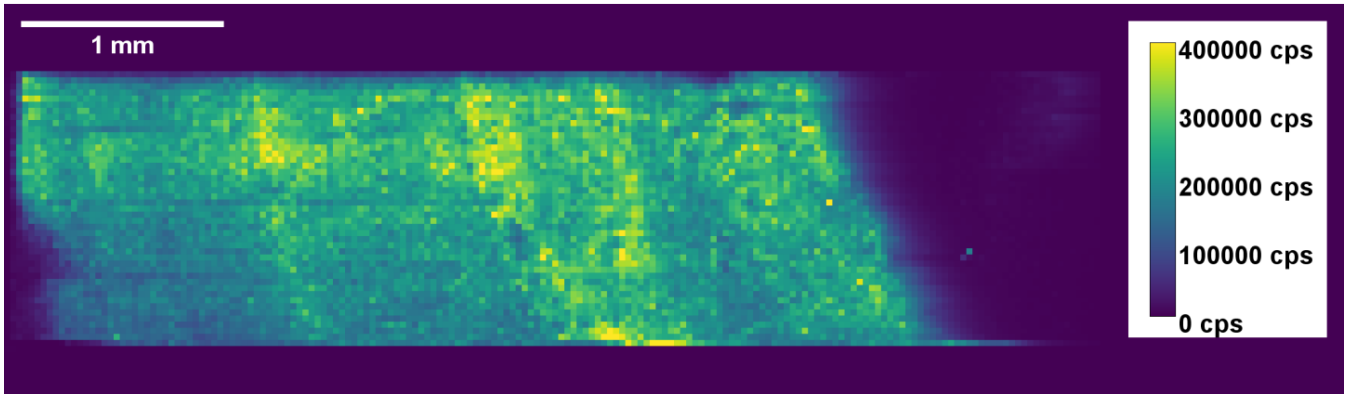

(b) $^{232}Th/^{238}U$

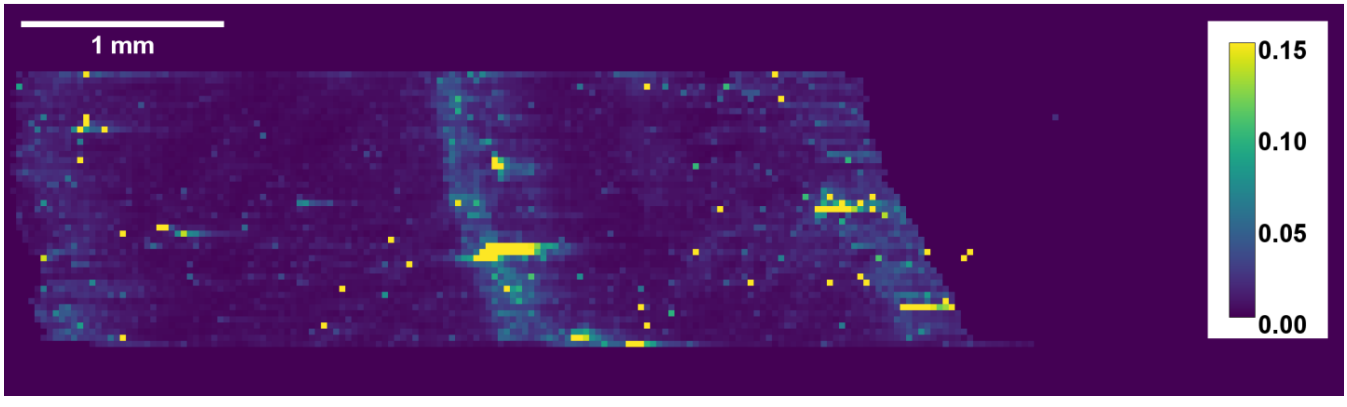

https://doi.org/10.5194/egusphere-2023-171
Preprint. Discussion started: 13 March 2023

Figure B2: sample SOY-19-02 Endo part. The grow of the calcite if from the top of the image to the bottom

a) ^{238}U (b)$^{232}Th/^{238}U$

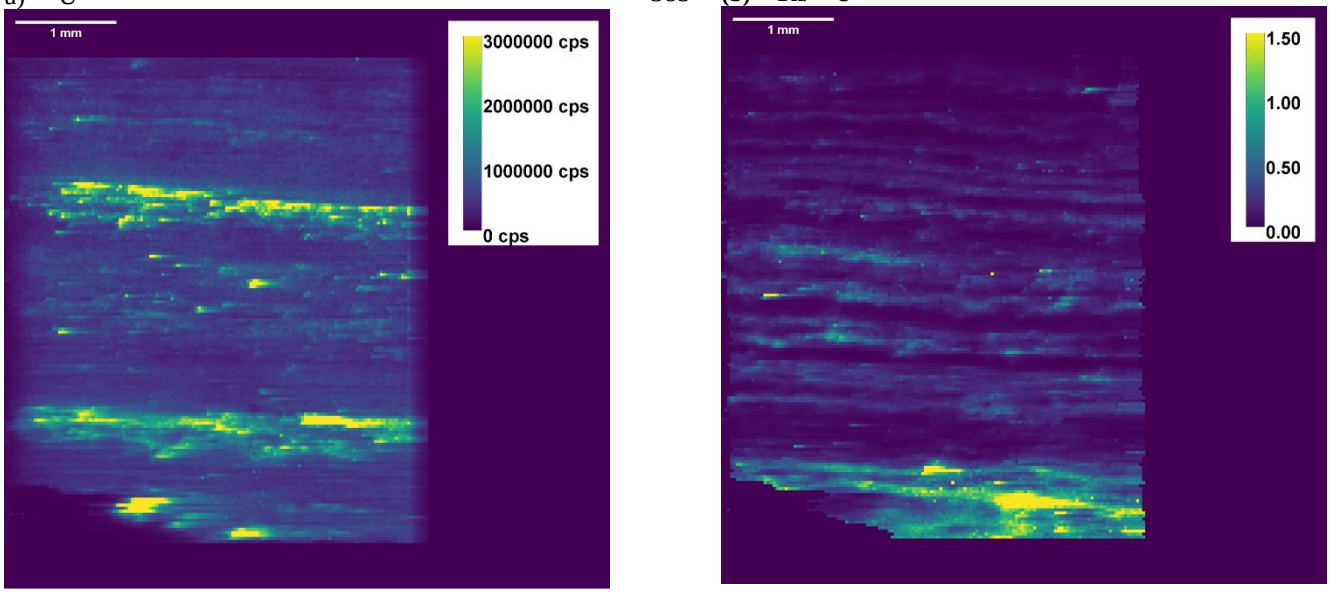

Figure B2: sample SOY-19-02 Exo part. The grow of the calcite if from the top of the image to the bottom

(a)^{238}U **(b)$^{232}Th/^{238}U$**

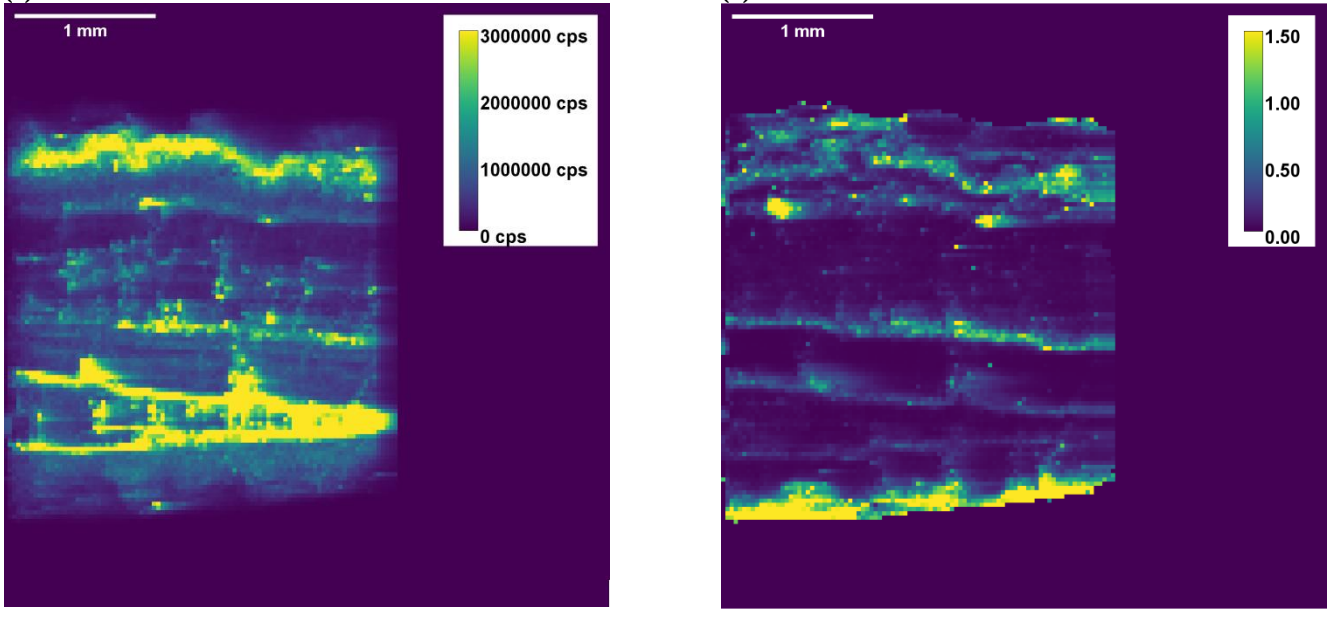

https://doi.org/10.5194/egusphere-2023-171
Preprint. Discussion started: 13 March 2023

Code availability

The STRUTages codes are available in Roy-Barmanand Pons-Branchu (2016). The codes used for calculating U-Th ages from fsLA- single collector-ICP-SFMS imaging are provided in Martin et al. (2022). All codes will be made available upon request to the authors.

Data availability

All data necessary to the study have been included. Any other data will be made available upon request to the authors.

Sample availability

All remaining samples will be made available upon request to the authors.

Author contribution

HV conceptualized the project, acquired funding for it and supervised it. FD and BG provided the study material. JN and BJ conducted the petrographic analysis. AD and EPB conducted the Liq-MC-ICPMS analysis. LM, GB, FC and CP performed the fsLA-ICPMS analysis under the supervision of CP. LM synthesized the data and prepared the original draft of the manuscript, which was reviewed and edited by JN, EPB, BJ, CP, NM and HV.

Competing interests

The authors declare that they have no conflict of interest.

Acknowledgments

This study was funded by the ANR through the APART project Grant number ANR-18-CE27-0004-01. We thank Rachel Roche Héritier of the musée archéologique of Soyons for welcoming and guiding us through the cave. The authors thank the PANOPLY analytical platform.

https://doi.org/10.5194/egusphere-2023-171
Preprint. Discussion started: 13 March 2023

References

Andersen, F.A. and Brečević, L.: Infrared spectra of amorphous and crystalline calcium carbonate, Acta Chem. Scand., 45, 1018–1024, doi:10.1002/chin.199209005, 1992.

Argant, A.: Rapport d'étude « Réseau Ursus » à Soyons (Ardèche), 12 pages, unpublished, 2010.

Bronk Ramsey, C: Radiocarbon calibration and analysis of stratigraphy: the OxCal program, Radiocarbon 37(2), 425–30, doi:10.1017/S0033822200030903, 1995.

Cailhol, D., Audra, Ph.: Contexte géomorphologique des grottes de Soyons (Ardèche), proceedings of the "23e Rencontre d'Octobre" (Le Châtelard, France, 12-13 October 2013), 2014.

Defleur, A. , White, T., Valensi, P., Slimak, L. and Crégut-Bonnoure, É.: Neanderthal Cannibalism at Moula-Guercy, Ardèche, France, Science, 286, 128–13, doi:10.1126/science.286.5437.128, 1999

Dumoulin JP., Comby-Zerbino C., Delqué-Količ E., Moreau C., Caffy I., Hain S., Perron M, Thellier B., Setti V., Berthier B. and Beck, L.: Status report on sample preparation protocols developed at the LMC14 Laboratory, Saclay, France: from sample collection to 14C AMS measurement, Radiocarbon, 59(3), 713-726, doi: 10.1017/RDC.2016.116, 2017.

Hellstrom, J.: U-Th dating of speleothems with high initial 230Th using stratigraphical constraint, Quat. Geochronol., 1(4), 289–295, doi: 10.1016/j.quageo.2007.01.004, 2006.

Huang C.K. and Kerr P.F.: Infrared study of the carbonate minerals, Am. Min., 45, 311–324, doi: , 1960.

Martin, L., Galy, A., Barbotin, G., Claverie1, F., Pons-Branchu, E., Tribolo, C., Mercier, N. and Pécheyran, C.: Isotopic Imaging using fs-LA HR-ICPMS for direct U/Th dating of small archaeological carbonates, Anal. Chem., 94(7), 3046–3055, doi:10.1021/acs.analchem.1c02241, 2022.

Mook WG. and Van Der Plicht J.: Reporting ^{14}C activities and concentrations. Radiocarbon, 41(3), 227–239, doi:10.1017/S0033822200057106, 1999.

Moreau, C., Messager, C., Berthier, B., Hain, S., Thellier, B., Dumoulin, JP., Caffy, I, Sieudat, M. and Beck, L.: ARTEMIS, The ^{14}C AMS facility of the LMC14 National Laboratory: a status report on quality control and microsample procedures. Radiocarbon, 62(6), 1755–1770, doi: 10.1017/RDC.2020.73, 2022.

Perrin, C., Prestimonaco, L., Servelle, G., Tilhac, R., Maury, M. and Cabrol, P.: Aragonite–calcite speleothems: identifying original and diagenetic features. J. Sediment. Res., 84(4), 245–269, doi:10.2110/jsr.2014.17 , 2014.

Pike, A. W., Hoffmann, D. L., García-Diez, M., Pettitt, P. B., Alcolea, J., De Balbin, R., González-Sainz, C., de las Heras, C., Lasheras, J.A., Montes, R., and Zilhão, J.: U-series dating of Paleolithic art in 11 caves in Spain. Science, 336(6087), 1409–1413, doi:10.1126/science.1219957, 2012.

Plagnes, V., Causse, C., Fontugne, M., Valladas, H., Chazine, J.-M. and Fage, L.-H.: Cross dating (Th/U-^{14}C) of calcite covering prehistoric paintings in Borneo. Quat. Res., 60, 172–179, doi:10.1016/S0033-5894(03)00064-4, 2003

Pons-Branchu, E., Douville, E., Roy-Barman, M., Dumont, E., Branchu, E., Thil, F., Frank, N., Bordier, L. and Borst W.: A geochemical perspective on Parisian urban history based on U-Th dating, laminae counting and yttrium and REE

https://doi.org/10.5194/egusphere-2023-171
Preprint. Discussion started: 13 March 2023

concentrations of recent carbonates in underground aqueducts. Quat. Geochronol., 24, 44–53, doi:10.1016/j.quageo.2014.08.001 , 2014.

Pons-Branchu, E. Sanchidrian, J.L., Fontugne, M., Medina-Alcaide, M.A., Quiles, A., Thil, F. and Valladas H.: U-series dating at Nerja cave reveal open system. Questioning the Neanderthal origin of Spanish rock art, J. Archaeol. Sci., 117, 105120, doi:10.1016/j.jas.2020.105120, 2020.

Reimer, P.J., Austin, W.E.N., Bard, E., Bayliss, A., Blackwell, P.G., Ramsey, C.B., Butzin, M., Cheng, H., Edwards, R.L., Friedrich, M., Grootes, P.M., Guilderson, T.P., Hajdas, I., Heaton, T.J., Hogg, A.G., Hughen, K.A., Kromer, B., Manning, S.W., Muscheler, R., Palmer, J.G., Pearson, C., van der Plicht, J., Reimer, R.W., Richards, D.A., Scott, E.M., Southon, J.R., Turney, C.S.M., Wacker, L., Adophi, F., Büntgen, U., Capano, M., Fahrni, S., Fogtmann-Schulz, A., Friedrich, R., Köhler, P., Kudsk, S., Miyake, F., Olsen, J., Reinig, F., Sakamoto, M., Sookdeo, A. and Talamo, S.: The IntCal20 Northern Hemisphere radiocarbon calibration curve (0-55 kcal BP), Radiocarbon, 62, 725–757, doi:10.1017/RDC.2020.41, 2020.

Sanchidrián, JL, Valladas, H, Medina – Alcaide, M.A., Pons-Branchu, E. and Quiles A.: New perspectives for 14C dating of parietal markings using CaCO3 thin layers: an example in Nerja cave (Spain). J. Archaeol. Sci. Rep., 12, 74–80, doi:10.1016/j.jasrep.2017.01.028 , 2017.

Roy-Barman, M. and Pons-Branchu, E.: Improved U-Th dating of carbonates with high initial ^{230}Th using stratigraphical and coevality constraints, Quat. Geochronol., 32, 29–39, doi:10.1016/j.quageo.2015.12.002, 2016.

Scholz, D., Tolzmann, J., Hoffmann, D. L., Jochum, K. P., Spötl, C. and Riechelmann, D. F.: Diagenesis of speleothems and its effect on the accuracy of 230Th/U-ages. Chem. Geol., 387, 74–86, doi:10.1016/j.chemgeo.2014.08.005 , 2014.

Spooner, P. T.; Chen, T.; Robinson, L. F. and Coath, C. D.: Rapid uranium-series age screening of carbonates by laser ablation mass spectrometry. Quat. Geochronol., 31, 28–39, doi:10.1016/j.quageo.2015.10.004, 2016.

Valladas, H, Pons-Branchu, E., Dumoulin, J.-P., Quiles, A., Medina-Alcaide, M.A. and Sanchidrain J.-L.: U/Th and C-14 cross dating of parietal calcite deposits: application to Nerja cave (Andalusia, Spain) and future perspectives. Radiocarbon 59 (6). 1955–1967, doi:10.1017/RDC.2017.120 , 2017.